

# Development of a 125 kW AMB Expander/Generator for Waste Heat Recovery

**Lawrence A. Hawkins**

e-mail: lhawkins@calnetix.com

**Lei Zhu**

e-mail: lzhu@calnetix.com

Calnetix, Inc.,  
23695 Via Del Rio,  
Yorba Linda, CA 92887

**Eric J. Blumber**

Calnetix Power Solutions, Inc.,  
23695 Via Del Rio,  
Yorba Linda, CA 92887  
e-mail: eblumber@calnetix.com

*The development and testing of an integrated power module (IPM) for a waste heat recovery system is described. The IPM is part of a waste heat recovery system based on the organic Rankine cycle. The waste heat system can recover energy from a wide variety of heat sources including landfill gas, reciprocating engine exhaust, solar, geothermal, boilers, and other industrial processes. The IPM incorporates a high performance, high speed permanent magnet generator with an integrated expansion turbine and low loss magnetic bearings. The IPM operates between 20,000 rpm and 26,500 rpm depending on the energy available from the heat source. The varying frequency voltage supplied by the generator is connected to the grid using an active/active power electronics package that can deliver power at 400–480 V<sub>ac</sub> (50 Hz or 60 Hz). Active magnetic bearings (AMBs) were chosen for the application because they can operate directly in the working fluid, have low losses, and provide high reliability and remote monitoring capabilities. This system has a flow-through design and an inboard impeller layout that produces desirable rotordynamics for a simple magnetic bearing control. An extensive shop testing procedure is described, and measurements and predictions are presented, showing good correlation. Shop testing of the IPM in the waste heat system has been completed for 15 systems. The magnetic bearings and backup bearings have performed as designed. The thrust balancing system has limited the thrust load that must be reacted by the axial magnetic bearings to 25% of the design load capacity in the worst case. The first field unit was installed in April 2009 at a biogas site. [DOI: 10.1115/1.4002660]*

*Keywords:* active magnetic bearings, waste heat recovery, waste heat generator

## 1 Introduction

The expander/generator (referred to below as the IPM or IPM125) is the key component of a 125 kW (net) waste heat recovery system that utilizes a heat input of at least 835 kW and temperature of 110°C (230°F) or higher to generate electricity to the grid. A process flow diagram for the waste recovery system is shown in Fig. 1. The working fluid is a high molecular weight organic fluid with a much lower boiling point than water, allowing heat recovery from low temperature sources. The system, referred to here as a waste heat generator (WHG), is factory built on a skid that is delivered to a site where waste heat is available (Fig. 2). The skid is connected on site to the heat source (evaporator in Fig. 1), to a condensing source (condenser in Fig. 1), and to the electrical grid. Due to the modular design of the skid, the heat input can be designed for a variety of direct and indirect heat sources. Direct heat sources provide heat directly to the refrigerant using a single facility heat exchanger. A waste gas burner with a heat exchanger carrying the working fluid would be an example of a direct heat source. Heat sources can also be indirect where a secondary fluid is required to carry heat to the refrigerant. This configuration requires two facility heat exchangers but allows for a more compact refrigerant loop.

The waste heat recovery system operates in a closed-loop organic Rankine cycle (ORC) using a HFC-R245fa refrigerant as a working fluid. The basic steps in the cycle are itemized below, following the nomenclature in Fig. 1.

- Starting at the receiver, the working fluid is a liquid at the condensing pressure and temperature.
- The working fluid enters the pump where the pressure is raised to the evaporating pressure.
- The working fluid passes through a heat exchanger (economizer) to take heat out of the gas leaving the IPM125 expander module—this improves overall system efficiency.
- The working fluid is now a warmer, high pressure liquid. The working fluid then enters the evaporator, where it is exposed to waste heat via a heat exchanger, which evaporates the fluid to a high pressure vapor.
- The working fluid (now a vapor) enters the turbine of the IPM125. Driven by the pressure, the IPM125 generator and associated power electronics convert this energy to electrical power (voltage and current at the spin frequency) that can be directly connected to the grid at 50 Hz or 60 Hz.
- The working fluid still has considerable heat, some of which is transferred to the pumped liquid in the economizer. This helps in two ways: (1) This heat would have otherwise been extracted in the condenser, and (2) there is less heat required at the evaporator due to the liquid being prewarmed.
- The working fluid (still a vapor) then flows to the condenser where heat is extracted and the working fluid condenses to a liquid. The low pressure, liquid working fluid drains back to the receiver to complete the cycle.

## 2 IPM

The IPM, shown in cross section in Fig. 3, is the core of the WHG system. It combines a high speed permanent magnet (PM) generator with a centrifugal expansion turbine supported on magnetic bearings. The generator is connected to a power electronics (PE) package that converts the variable frequency IPM output power for grid connectivity with –50 Hz and 400 V or 60 Hz and

Contributed by the International Gas Turbine Institute (IGTI) of ASME for publication in the JOURNAL OF ENGINEERING FOR GAS TURBINES AND POWER. Manuscript received May 9, 2010; final manuscript received May 12, 2010; published online March 16, 2011. Editor: Dilip R. Ballal.

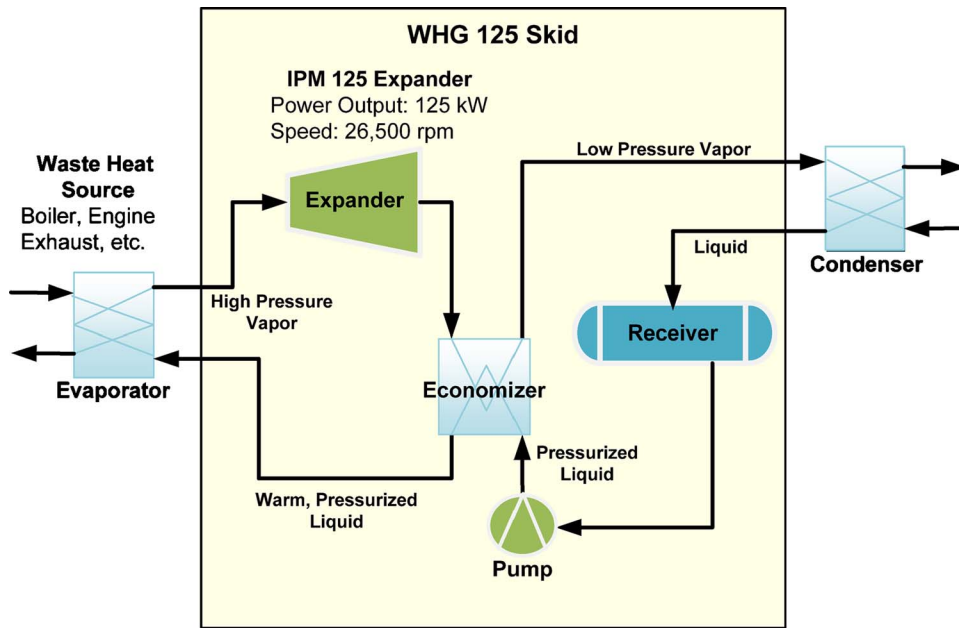


Fig. 1 WHG process flow diagram

480 V. The IPM produces full power at its normal operating speed of 26,500 rpm but can output a reduced power level down to 20,000 rpm. This is an important feature because the energy available from many waste sources varies considerably throughout the day or from day to day. The rotordynamics and magnetic bearing controls are sufficiently robust to allow stable and smooth operation at any speed from 0 rpm up to the 25% overspeed of 33,125 rpm.

The IPM is of a flow-through design, allowing it to be installed in the middle of a straight run of pipe. Superheated refrigerant enters from the right in Fig. 3 and is directed into an annular space by the diverter cone. A typical inlet condition is 121 °C (250 °F) and 1.72 MPa (250 psi). The gas then flows radially inward through a nozzle into the turbine. Expansion across the turbine results in a temperature drop and an 8:1 pressure drop. The exhaust then passes through the generator rotor/stator air gap and

around the outside of the generator stator to provide cooling for the generator. The expander/generator can convert up to 145 kW to terminal power and deliver a net 125 kW to the grid after losses in the PE and losses for auxiliary equipment (pump, control, etc.). The overall efficiency of heat input to grid power is approximately 12–16%, depending on the temperature of the waste heat stream and the condensing wet bulb temperature. As a typical example, with a waste heat gas stream of 900 kW (3.1 MBtu/h) and 300 °F, the IPM can deliver a net 125 kW to the grid.

The generator uses a two-pole, radially polarized PM rotor. The magnets are constrained by a thick nonmagnetic retaining sleeve, which also provides the structural connection between the generator and the rest of the machine. PM machines use permanent magnets to provide field excitation, providing high efficiency and reduced size for an equivalent power when compared with induction and variable reluctance machines. They also have lower rotor

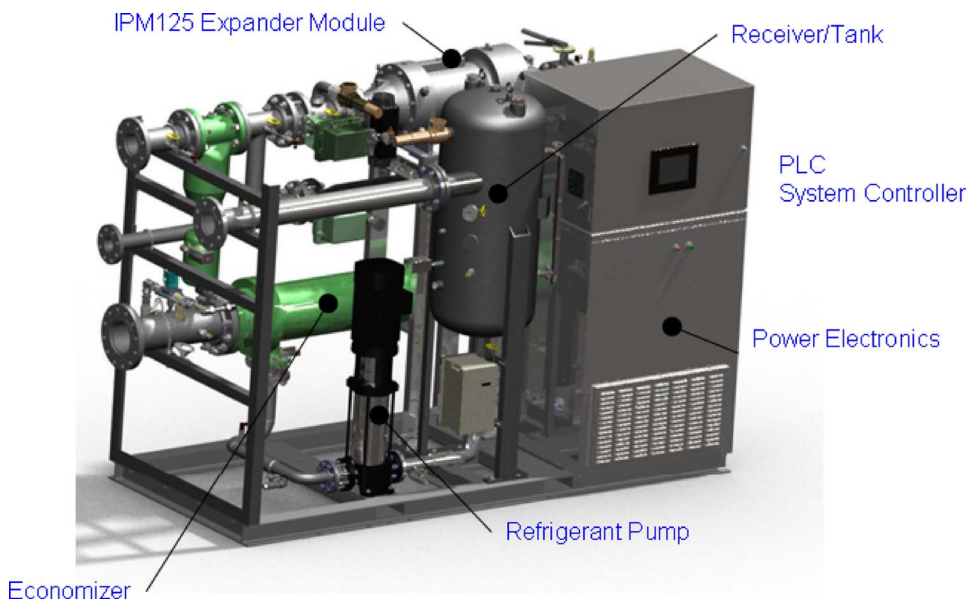


Fig. 2 Calnetix WHG125 prepackaged skid

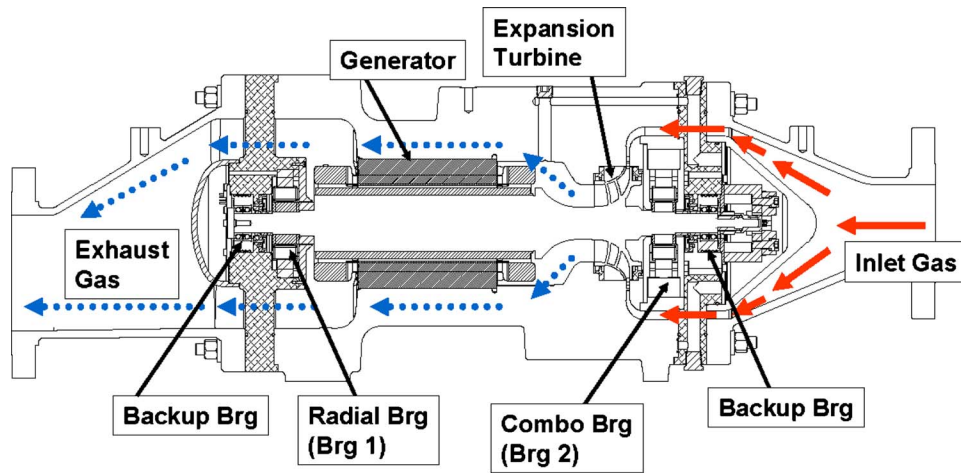


Fig. 3 Cross section of the IPM

losses and lower winding inductances, which make them suitable for the rapid energy transfer in expander applications. The three-phase stator is conventionally wound, allowing a simple, low cost construction.

The output of the expander/generator is connected to an active/active PE package. The power electronics package uses an insulated gate bipolar transistor (IGBT) rectifier to convert the variable frequency, high voltage output from the expander/generator to DC. It then converts the DC to  $400 V_{ac}/480 V_{ac}$  at 50 Hz/60 Hz for power delivery to the grid. Flexibility and adaptability are provided by digital control software that implements the control algorithms that have been proven through system modeling and simulation.

A key design feature of the IPM is the location of the expander inboard of the bearings. This has several benefits as follows: (1) enables the flow-through design, making the WHG skid space efficient and easy to assemble, (2) exhaust gas exiting over the generator provides cooling for the generator, and (3) rotor flexible modes have a very small gyroscopic effect, resulting in much simpler magnetic bearing control (the expander would otherwise have an overhung impeller and would be gyroscopic).

**2.1 Bearing Selection.** During the design and development of the IPM, several different bearing options were explored: (1) ball bearings with oil lubrication, working fluid lubrication, and grease lubrication, (2) sleeve or tilt pad bearings with working fluid lubrication, and (3) magnetic bearings. The oil lubricated ball bearings would have required a very complicated sealing arrangement that would have defeated the purpose of the integrated design. Working fluid lubricated would not have adequate life due to the poor lubricating properties of the expected working fluids. Grease lubricated ball bearings would not have adequate grease life or bearing life due to the lack of cooling and the relatively high working temperature. Working fluid lubricated fluid film bearings would have high losses and limited life.

Magnetic bearings were chosen because they do not require lubrication and allow for near frictionless operation and no wear, thereby optimizing the efficiency and reliability of the system (there is no contact between the rotating assembly and the bearings). The rotor power loss from eddy currents and windage at the bearing journals was estimated to be less than 35 W at operating speed. Other benefits are that the bearings do not require their own cooling system, they have remote monitoring and diagnostic capability, and there is no need to isolate the working fluid from the generator and bearings. This last feature allows the entire module to be hermetically sealed, minimizing the potential for working fluid leakage outside of the system.

**2.2 Thrust Balancing.** Another key feature of the IPM is the use of the impeller as a balance piston to minimize the aerodynamic thrust load that must be reacted by the bearings. The sealing and thrust balancing scheme are illustrated in Fig. 4. The inboard seal at the impeller exit prevents high pressure inlet gas from bypassing the impeller. The outboard seal on the back plane of the impeller minimizes the leakage of high pressure gas into the bearing compartment. Without the seal, the pressure on the entire outboard side of the impeller would be near the 1.72 MPa inlet pressure, much higher than the pressure across the exit plane of the impeller, resulting in a net load of about 10.7 kN (2400 lbf). To react this load directly would require a very large thrust bearing and would result in undesirable dynamics and packaging issues.

The choice of the seal type is also important. Design considerations were (1) tolerance to static and dynamic offset in both the radial and axial directions, (2) long life with minimal losses at normal operating speed, (3) leakage less than 1% of the working fluid flow rate, (4) ability to withstand 2.0 MPa (300 psi) delta pressure and 149°C (300°F), and (5) initial cost. Based on these requirements, several seals were considered for the design including (1) stepped labyrinth, (2) floating carbon ring, (3) brush, and (4) carbon face seal. Brush seals were chosen for the prototype machines and for the first production release because previous experience gave the highest level of confidence in accomplishing all of the performance objectives on the initial design. Other seal designs will be investigated during a future cost reduction phase of the machine.

None of the seals that were considered are zero leakage seals. Typically a double seal with buffering is required to get zero

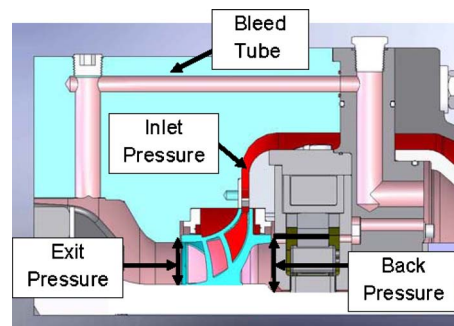


Fig. 4 Thrust balancing scheme for the IPM

**Table 1 Magnetic bearing characteristics**

Bearing	Radial bearing	Combo bearing (radial)	Combo bearing (axial)
Bearing reference name	Brg 1	Brg 2	Axial
Coordinate names	x1, y1	x2, y2	z
Load capacity, N (lbf)	316 (71)	521 (117)	1380 (310)
Force constant, N/A (lbf/A)	71 (16)	116 (26)	312 (70)
Negative stiffness, N/mm (lbf/in.)	1244 (7100)	1209 (6900)	1261 (7200)
Air gap, mm (in.)	0.508 (0.020)	0.635 (0.025)	0.762 (0.030)
Maximum current, A	3.2	3.2	5.5

leakage for a rotating seal, resulting in a more complicated and costly design and a higher axial space requirement (longer rotor). Therefore, a bleed pathway is used to vent the bearing compartment back to the exit of the expander. Without the bleed, a small amount of seal leakage would cause the pressure on the outboard side of the impeller to slowly build up to the inlet pressure, defeating the purpose of the seal. The bleed pathway allows the fluid leaking through the seal to reach the impeller exit with a small pressure drop. The resulting thrust load from static pressure has been found to be less than about 335 N (75 lbf) on new machines. The thrust load may slowly rise over long time periods due to future seal wear. Axial bearing coil current—and thus thrust load—will be trended in long term operation as a built-in monitoring test for possible seal wear.

**2.3 Magnetic Bearings.** The magnetic bearings use a homopolar, permanent magnet bias topology. Homopolar refers to the direction of the bias flux, which is oriented either uniformly into or uniformly out of the shaft at any circumferential location. This topology significantly reduces rotor eddy current losses compared with conventional designs. A permanent magnet is used to produce the bias flux for the bearing, resulting in several advantages compared with electromagnetic bias as follows: (1) Less power is consumed by the magnetic bearings, and (2) the bearing has a more linear force/displacement characteristic due to the contribution of the large, fixed reluctance of the permanent magnet to the bias flux path.

Brg 1 is a two-axis radial bearing. Brg 2, shown in Fig. 3, is a three-axis combination (combo) radial/thrust bearing. The basic operation of these two bearing topologies was described in Refs. [1,2]. Since the combination bearing is more compact axially than separate radial and axial magnetic bearings, the overall rotor length is reduced. This increases the frequency of the rotor bending modes, making the magnetic bearing control design less difficult. The combination bearing uses a single radially polarized permanent magnet ring to provide bias flux for both the radial and axial flux paths. Three separate pairs of control coils allow individual control of each axis (two radial and one axial).

Some characteristics of the magnetic bearings are given in Table 1. These characteristics are analytical values calculated with 95% lamination stack factor and 37 MG Oe permanent magnets at 21 °C (70 °F). The radial bearing load capacities are calculated for a load between poles. Measured thrust load capacity data are reported below in the discussion of IPM testing.

**2.4 Magnetic Bearing Control.** The radial magnetic bearing axes use differential laminated core reluctance sensors for detecting position. The axial magnetic bearing axis uses a single-sided ferrite core reluctance sensor. The sensors are driven by a 15 kHz drive signal that is modulated as the shaft motion changes the gap reluctance. The magnetic bearing control board has the drive circuit and six synchronous demodulation circuits, one for each of

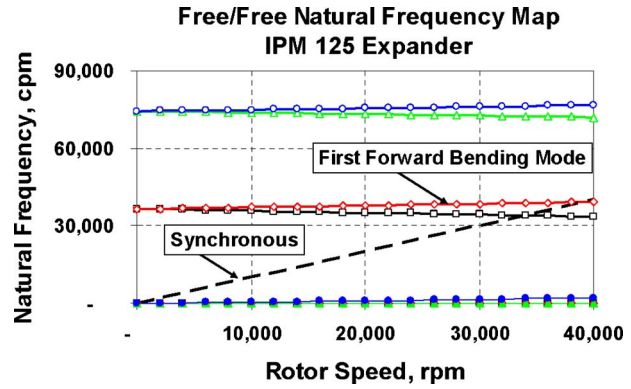


**Fig. 5 Free/free natural frequency map for the IPM rotor**

the five control axes and a spare for undefined future use. The sensor signals are fed to a TI F2812 digital signal processor (DSP) that executes the magnetic bearing control program.

The control for this machine is single-input, single-output (SISO) enhanced proportional-integral-derivative (PID). In addition to a basic PID compensator, the control has additional biquadratic filters to tailor the phase and gain frequency response to produce a robust, stable closed-loop control. Synchronous cancellation is used to minimize the response to unbalance from just below the rotor rigid body mode frequencies to above the maximum overspeed (33,125 rpm). The power consumed by the magnetic bearing control box—power for the electronics and the magnetic bearing actuators—varies from 60 W to 90 W depending on the load reacted.

**2.5 Backup Bearings.** A backup or auxiliary bearing system is used for rotor support during nonoperation of the magnetic bearings and for emergency spin-down of the rotor in the event of an overload or failure in some part of the magnetic bearing system. The exhaust end backup bearing set provides radial support only and the inlet end set provides both radial and thrust support for the rotor. The baseline configuration for each bearing set is a duplex pair of face/face mounted angular contact ball bearings (Fig. 2). The baseline bearings have standard 52100 steel races, ceramic balls, phenolic cage, and shields. The thrust backup bearing must carry any unbalance thrust load in the event of a loss of magnetic bearing control. The axial clearance is ±0.15 mm (0.006 in.). The radial clearance between the backup bearing inner race and the shaft sleeve is 0.13 mm (0.005 in.).

The backup bearings are mounted in a compliant mount that provides damping and sets the desired support stiffness. The arrangement is very similar to that described in Ref. [3]. The backup bearings have very generous design margins on speed and load capacity for this application. They were called into service several times during initial development of the WHG system control and performed as expected.

**2.6 Rotordynamics.** A rotordynamic and controls model was assembled for the IPM125 rotor and magnetic bearings. A free/free natural frequency map of the rotor is shown in Fig. 5. The first forward bending mode is about 36,600 cpm (610 Hz) at 0 rpm. This mode has a very weak gyroscopic effect because of the location of the impeller inboard of the bearings. At the normal operating speed of 26,500 rpm, the first forward bending mode is 38,500 cpm (642 Hz). This is a margin of 45% above the operating speed. Two characteristics of the machine that simplify the magnetic bearing control design are the weak gyroscopic effect and subcritical operation with wide margin to the lowest bending mode. The system is required to operate briefly at an overspeed condition of 33,125 rpm (125% of nominal). At this speed, the first bending mode frequency is 38,750 cpm (646 Hz), a margin of 17%. This is adequate for short term operation. The second back-

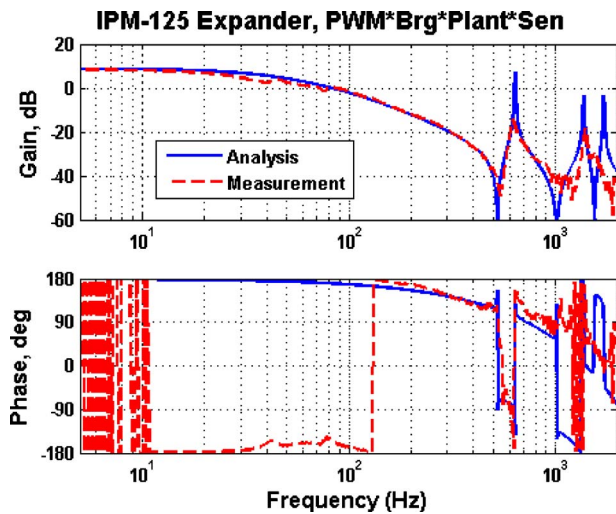


Fig. 6 Plant transfer function measurement, 0 rpm

ward and forward bending modes are above 75,000 cpm (1250 Hz). They must be addressed in the control design but are not a concern for synchronous response.

### 3 Shop Acceptance Testing of the IPM

A series of in-house tests is conducted before each IPM unit is shipped for installation in a WHG to verify the performance of the magnetic bearing system. The four main parts of the testing are the initial setup test, spin test, axial load test, and post-seal verification. The first three tests are conducted without the brush seals installed. After the brush seals are installed, a fourth abbreviated test is conducted to verify that no significant changes occurred as a result of seal installation. These tests are described below, along with some example measurements and predictions.

**3.1 Initial Setup Test.** In the initial setup test, resistance and inductance measurements are made for all the actuator and sensor coils. Also, resistance between all coils and the machine chassis and coil-to-coil resistance of adjacent radial actuator coils are measured to verify coil integrity. Then, there is a mechanical check to confirm the rotor axial travel in the backup bearings, followed by verification of the sensor to rotor target gaps for both the axial sensor and the speed sensor. After this, all radial and axial position sensors are calibrated using an automatic routine that is initiated through a LABVIEW based magnetic bearing graphical user interface (GUI).

With the rotor levitated, five transfer functions—plant, compensator, open loop, closed-loop, and sensitivity—are measured for each of the five active control axes. The relevance of these measurements in a magnetic bearing system is discussed in detail in Ref. [4]. The transfer functions are measured using an internal feature of the magnetic bearing control program. A stepped sine excitation is applied to the controller output of the axis of interest. Simultaneously, the input and output signals from the controller are demodulated synchronously with the excitation signal. A complex division produces the gain and phase of the transfer function of interest one frequency at a time.

An example of plant transfer function measurement is shown along with the predicted transfer function in Fig. 6. The correlation is quite good, particularly for the first two bending modes. To ensure good stability and robust performance, we require that the gain of each measured sensitivity transfer function be less than 10 dB in the measurement frequency range, following the ISO-14839-3 stability standard [5]. Figure 7 shows an example of measured sensitivity transfer function data compared with the pre-

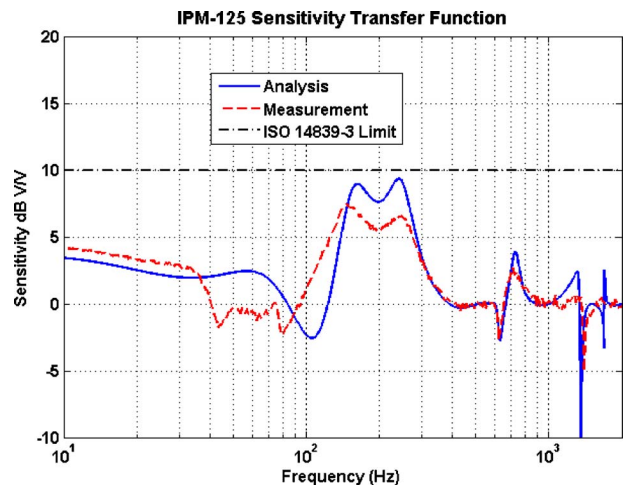


Fig. 7 Sensitivity transfer function measurement, 0 rpm

dicted model. As a verification of the hardware, we require the gain of the plant transfer function of radial X axis and combo radial X axis to be within 1 dB of their Y counterparts, respectively.

The DC coil currents required to support the static weight of the rotor (the levitation currents) are also recorded and compared with analytical values to ensure a good alignment of magnetic center and backup bearing center on each axis.

**3.2 Motoring Spin Test.** After passing the initial setup test, a spin test is conducted. The generator is used as a motor and is driven using the motoring mode of the PE. During the full speed, spin rotor position and coil current data are collected at a 5 kHz sample rate using the GUI. These high frequency data are reviewed to make sure no abnormal conditions appear during the test. Synchronous vibration data are also collected at every 250 rpm increment of spin speed. Synchronous displacement, current, and cancellation amplitude and phase are continuously calculated by the controller and are available through the GUI. For a new machine, we require that the synchronous orbit be less than 0.0254 mm (0.001 in.) 0 pk for both radial and combo radial bearings for any speed up to 26,500 rpm. This is 20% of the 0.127 mm (0.005 in.) backup bearing radial clearance, which is the minimum rotor to stator clearance. The ISO vibration standard, ISO-14839-2 [6], allows rotor motion, synchronous and nonsynchronous, of up to 30% (Zone A). Measured synchronous data for one unit are shown in Fig. 8. The five transfer functions men-

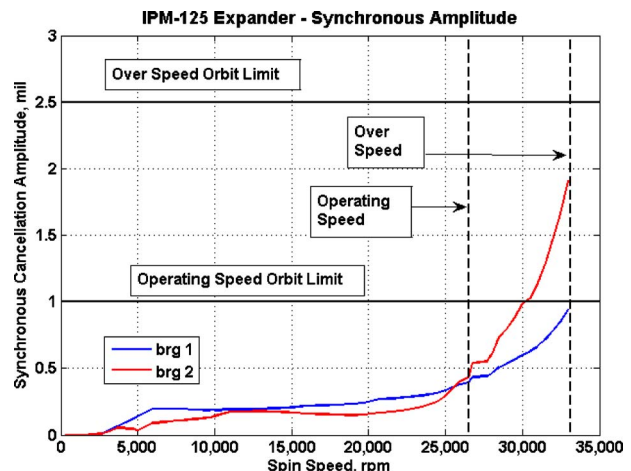


Fig. 8 Synchronous response data from the position sensors

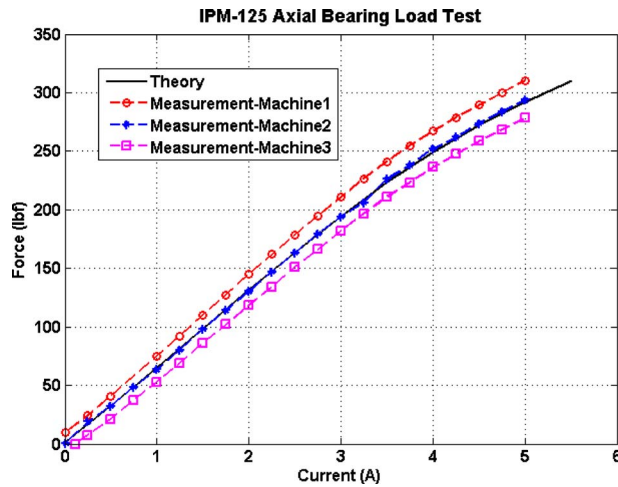


Fig. 9 Measured axial load versus current. Comparison of several measurements and theory.

tioned above are collected at 26,500 rpm for each axis, and the same sensitivity criteria are used. Under some trip conditions in the field application of the IPM, the unit may see a brief (less than 1 s) overspeed condition up to 33,125 rpm. Each unit is spun to this speed during in-house testing to verify control stability and rotor integrity. We require that the synchronous orbit be less than 0.0635 mm (0.0025 in.) at speeds from the 26,500 rpm operating speed to the 33,125 rpm overspeed.

**3.3 Axial Load Test.** Each machine is installed on a special load test platform that facilitates applying and measuring static axial or radial loads. The radial bearing load capacity is measured only on selected units because the dynamic radial load is small due to the use of synchronous cancellation, the static radial load is expected to be near constant over time, and the radial axes on IPM125 unit do not take heavy load. The axial load is measured on all units because it is anticipated but not yet observed in field testing that future long term seal wear may result in an axial load that increases over long time periods. Having an accurate axial load versus current characteristic for all units will assist in drawing better conclusions from future field data. The axial bearing is loaded in 0.25 A (A) steps until the axial coil current reaches 5.0 A. Both the axial coil current and the applied force are recorded and plotted. A plot of the force/current for one machine is given in Fig. 9 along with an analytical prediction using in-house analysis tools [2]. The slope of the force versus current curve is reasonably linear between 0.5 A and 3.5 A. We have found that the measured slope, or actuator gain, falls within  $385 \text{ N/A}$  ( $64 \text{ lbf/A}$ )  $\pm 10\%$ . This agrees well with the predicted value of  $385 \text{ N/A}$  ( $64 \text{ lbf/A}$ ). On selected units, an offset test is carried out in which a rotor is moved axially around the normal levitation point. When the offset is plotted versus the axial levitation current, the slope of the curve is the ratio between the force constant and the negative stiffness. A good estimate of the negative stiffness can be extracted from this ratio by using the force constant determined in the load test.

**3.4 Verification Tests With Seals Installed.** After the load test, the IPM is disassembled and the inboard (impeller exhaust) and outboard (back plane) brush seals are installed. With the seals installed, selected tests are repeated that were performed previ-

ously without the seals. These tests include the sensor calibration verification, 0 rpm transfer function measurements, recording of levitation currents, and a low speed spin test. Measured data are then reviewed, and if nothing unusual is found, the unit is shipped for installation in a WHG for final acceptance testing.

The brush seals do not have an obvious impact on the rotordynamic characteristics of the machine when spinning. Measured plant and closed-loop transfer functions with and without the seals are generally similar. At zero speed, the plant transfer function measurements for some machines will indicate that the brush seals are adding a small positive stiffness. This minor effect goes away after the machine is spun and returned to rest. This effect is apparently caused by some small friction between the brushes before they deflected a few times.

#### 4 WHG Installation

After shop testing, the IPM is assembled into the WHG skid. The complete skid is tested in a test cell with a controllable heat source (a boiler), providing the waste heat. Of 15 tested systems, the maximum thrust load—occurring generally at the maximum inlet pressure—has varied from negligible to just under 335 N (75 lbf).

The first field installation was in April 2009. The waste heat source is the exhaust from a digester at a waste water treatment plant. This unit has accumulated over 3500 h of operation as of December 2009. Operating results will be reported in a future forum.

#### 5 Conclusions

The development of an IPM for a waste heat recovery system was described. Magnetic bearings were chosen for this application because of their low losses, high reliability, long life, and ability to operate directly in the working fluid (a refrigerant) without lubrication. This system has a flow-through design and an inboard impeller layout that produces desirable rotordynamics for a simple magnetic bearing control. An extensive shop testing procedure was described, and test and predicted measurements were presented, showing good correlation. Shop testing of the IPM in the waste heat system has been completed for 15 systems. The magnetic bearings and backup bearings have performed as designed. The thrust balancing system has limited the thrust load that must be reacted by the axial magnetic bearings to 25% of design load capacity in the worst case.

#### References

- [1] McMullen, P., Huynh, C., and Hayes, R., 2000, "Combination Radial-Axial Magnetic Bearing," *Proceedings of the Seventh International Symposium on Magnetic Bearings*, Zurich, Switzerland.
- [2] Filatov, A. V., McMullen, P. T., Hawkins, L. A., and Blumber, E., 2004, "Magnetic Bearing Actuator Design for a Gas Expander Generator," *Proceedings of the Ninth International Symposium on Magnetic Bearings*, Lexington, KY.
- [3] Hawkins, L., McMullen, P., and Vuong, V., 2007, "Development and Testing of the Backup Bearing System for an AMB Energy Storage Flywheel," ASME Paper No. GT2007-28290.
- [4] Schweitzer, G., and Maslen, E. H., 2009, *Magnetic Bearings*, Springer-Verlag, Berlin, pp. 61–67.
- [5] International Standard ISO 14839-3:2006, "Mechanical Vibration—Vibration of Rotating Machinery Equipped With Active Magnetic Bearings—Part 3: Evaluation of Stability Margin," International Organization for Standardization.
- [6] International Standard ISO 14839-2:2004, "Mechanical Vibration—Vibration of Rotating Machinery Equipped With Active Magnetic Bearings—Part 2: Evaluation of Vibration," International Organization for Standardization.